

# Effect of slip flow on pressure drop of nanofiber filters

メタデータ	言語: eng 出版者: 公開日: 2017-12-28 キーワード (Ja): キーワード (En): 作成者: メールアドレス: 所属:
URL	<a href="https://doi.org/10.24517/00049629">https://doi.org/10.24517/00049629</a>

This work is licensed under a Creative Commons Attribution 3.0 International License.



## **Effect of slip flow on pressure drop of nanofiber filters**

**Hyun-Jin Choi<sup>a,b</sup>, Mikio Kumita<sup>a,\*</sup>, Takafumi Seto<sup>a</sup>, Yuki Inui<sup>c</sup>, Li Bao<sup>d</sup>, Toshiyuki Fujimoto<sup>e</sup>, Yoshio Otani<sup>a</sup>**

<sup>a</sup> *Institute of Science and Engineering, Kanazawa University, Kakuma-machi, Kanazawa, Ishikawa 920-1192, Japan*

<sup>b</sup> *Environmental Assessment Group, Korea Environment Institute, 370 Sicheong-daero, Sejong 30147, Republic of Korea*

<sup>c</sup> *Graduate School of Science and Technology, Kanazawa University, Kakuma-machi, Kanazawa, Ishikawa 920-1192, Japan*

<sup>d</sup> *Nippon Muki Co., Ltd., 5-1-5 Higashi-Ueno, Taito-ku, Tokyo 110-0015, Japan*

<sup>e</sup> *Department of Applied Sciences, Muroran Institute of Technology, 27-1 Mizumoto-cho, Muroran, Hokkaido 050-8585, Japan*

\* Corresponding author. Mikio Kumita

*E-mail address:* kumita@se.kanazawa-u.ac.jp (M. Kumita).

*Tel.:* +81 76 234 4827; *fax:* +81 76 234 4826

## **ABSTRACT**

The slip flow effect is often brought out to explain the reduction in pressure drop for nanofiber filters. Kirsch et al. (1973) studied the slip flow effect on the pressure drop of fibrous filters consisting of micron fibers, and proposed an empirical equation to predict the dependence of the dimensionless drag,  $F$ , on the Knudsen number,  $Kn$ , with considering non-uniformity of fiber packing. However, their empirical equation was derived based on the experiments with filters consisting of micron fibers so that the empirical equation is not yet verified for nanofiber filters. In the present work, we used various commercially available nanofiber filters with various physical properties, and the pressure drop was measured at low pressures in order to examine the validity of the empirical equation. As a result, we found that the empirical equation is valid even for nanofiber filters with a large inhomogeneity factor at a large  $Kn$  up to 20.

**Keywords:** Air filtration, Slip flow, Nanofiber filter, Inhomogeneity factor, Knudsen number

## 1. Introduction

Air filters play important roles in various fields such as air cleaning, particle sampling, and respiratory protection due to its high collection efficiency, simple structure, and economical cost as well as a low pressure drop (Zhang et al., 2010; Sambaer et al., 2011; Leung and Hung, 2012; Wang and Otani, 2013; Choi et al., 2015; Li et al., 2015). The initial filtration performance is evaluated by the filter quality factor,  $q_F$ , defined as the ratio of logarithm of particle penetration to the pressure drop (Hinds, 1999):

$$q_F = -\ln P/\Delta p \quad (1)$$

where,  $P$  is the particle penetration, and  $\Delta p$  is the pressure drop across the filter media. Since, a good filter media has a high collection efficiency and a low pressure drop (Hung and Leung, 2011; Bao et al., 2016), it has a higher value of  $q_F$ . Therefore, air filters made of nanofibers have attracted a great attention because they may simultaneously achieve a high collection efficiency due to diffusion and interception and a low pressure owing to the slip flow effect (Bao et al., 2016).

The flow around a fiber is classified into three regimes, namely, molecular flow regime, transitional flow regime and continuous flow regime, according to the Knudsen number,  $Kn = 2\lambda/d_f$ , where  $\lambda$  is the mean free path of air and  $d_f$  is the fiber diameter (Brown, 1993; Barhate and Ramakrishna, 2007; Pich, 1971). When a fiber diameter is small and comparable to the mean free path of air, Knudsen number becomes close to unity and the air flow around a fiber behaves like a rarefied gas. In the transitional regime, the boundary condition of flow velocity on the fiber surface is assigned as a non-zero velocity (slip flow condition), which results in a lower pressure drop (Barhate and Ramakrishna, 2007; Sambaer et al., 2011; Bao et al., 2016). Although the slip flow effect is commonly accepted in the aerosol filtration, there have been few studies on the influence of slip flow on the pressure drop. Kirsch et al. (1973) measured the pressure drop at low pressures using micron-fiber filters and proposed an empirical equation to predict the dependence of the dimensionless drag,  $F$ , on the Knudsen number,  $Kn$ , accounting for the non-uniformity of fiber packing and the packing density. However, their empirical equation was obtained based on the experiments with filters consisting of micron fibers so that the validity of proposed empirical equation is not assured for nanofiber filters.

In the present work, we prepared the nanofiber filters with various physical properties, and the pressure drop was measured at low pressures in order to examine the validity of empirical equation proposed by Kirsch et al. (1973).

## 2. Slip flow effect on the pressure drop of fibrous filters - Kirsch et al. (1973)

As the fiber size decreases to nanometer-scale, the slip flow on the fiber surfaces becomes significant and the pressure drop is expected to be low compared to that without the slip flow. Kirsch et al. (1973) experimentally investigated the influence of slip flow on the dimensionless drag,  $F$ , for real filters, proposed

the following empirical equation:

$$F^{-1} = F_0^{-1} + \frac{\tau\varphi}{4\pi}(1-\alpha)Kn \quad (2)$$

where,  $F_0$ , is the dimensionless drag without the slip flow ( $Kn = 0$ ),  $\tau = 1.43$  is the slip coefficient,  $\varphi$  the function of filter structure, and  $\alpha$  the packing density. Furthermore, they empirically determined  $\varphi = \delta^{1/2}$  as a function of the inhomogeneity factor,  $\delta$ . The inhomogeneity factor,  $\delta$ , is defined as the ratio of dimensionless drag of a fan model filter, FMF, to that of a real filter with same packing density at  $Kn = 0$ :

$$\delta = \left( \frac{F^m}{F^r} \right)_{Kn=0} \quad (3)$$

$$F^m = 4\pi/k \quad (4)$$

$$k = -0.5 \ln \alpha - 0.52 + 0.64\alpha + 1.43(1-\alpha)Kn \quad (5)$$

where,  $k$  is the hydrodynamic factor, and the superscripts m, r represents “model” and “real” respectively.

**Table 1** shows the physical properties of filters studied by Kirsch et al. (1973). As shown in the table, the fiber diameter studied was larger than  $3 \mu\text{m}$  since there existed no nanofiber filters in 1970's. They measured the pressure drop at various low pressures (760 to 7 mmHg), and calculated the dimensionless drag of filter,  $F$ , by the following equation:

$$F = \frac{\Delta p}{\mu ul(1-\alpha)} \quad (6)$$

$$l = \frac{4\alpha L}{\pi d_f^2} \quad (7)$$

where  $l$  is the fiber length in unit filter area,  $u$  the filtration velocity,  $L$  the filter thickness, and  $d_f$  the fiber diameter. **Fig. 1** shows how they obtained the empirical equation of Eq. (2). They plotted the reciprocal of experimental dimensionless drag of filters No. 1–4 (the same fiber mat but with different packing densities) calculated by Eq. (6) against Knudsen number (Fig. 1(a)), and the slopes of these lines, which corresponds to  $\tau\varphi(1-\alpha)/4\pi$  are plotted against  $1-\alpha$  (Fig. 1(b)) so as to find that the coefficient of  $Kn$  is proportional to  $1-\alpha$ . Then the slope divided by  $1-\alpha$ , which corresponds to  $\tau\varphi$ , was plotted against  $\delta$  to find  $\varphi = \delta^{1/2}$  (Fig. 1(c)).

However, the empirical equation of Eq. (2) was based on the experimental data for microfiber filters so that the validity for nanofiber filters should be examined. In the present work, we measured the pressure drop of nanofiber filters at various low pressures and studied the dependence of dimensionless drag of

nanofiber filters on Knudsen number,  $Kn$ , the packing density,  $\alpha$ , and the inhomogeneity factor,  $\delta$ .

### 3. Experimental setup and method

#### 3.1 Test filters

Eight commercial nanofiber filters with various physical properties were used in the present work. The fiber diameter,  $d_f$ , was measured by counting more than 200 fibers observed with the field emission scanning electron microscope (FE-SEM) (S-4500, Hitachi, Ltd., Japan). The packing density of filters,  $\alpha$ , was calculated by the following equation:

$$\alpha = \frac{W}{L\rho} \quad (8)$$

where  $\rho$  is density of fibers,  $L$  is the filter thickness measured by a micrometer, and  $W$  the filter area density. The physical properties of test filters are given in **Table 2**.

#### 3.2 Measurement of pressure drop at low pressure conditions

**Fig. 2** shows the experimental setup to measure the pressure drop at the low pressures. An orifice with diameter of 0.7 mm was placed upstream of the test filter. The pressure of the system was reduced using a vacuum pump connected downstream of the test filter. The volumetric flow rate increases until the flow through the orifice reaches the critical, and after the critical, the filtration velocity increases with decreasing the pressure while the mass flow remains the same. The mass flow rate was measured using a mass flow meter (MFM) (Model 4043, TSI Inc., USA) at the ambient pressure. The pressure drop was measured by a differential monometer (Testo 510, Testo AG, Germany).

### 4. Results and discussion

**Fig. 3(a)** shows the pressure drop of test filters as a function of absolute pressure. As shown in the figure, the pressure drop increases with decreasing the absolute pressure because the filtration velocity increases inversely proportional to the absolute pressure after the pressure downstream of the orifice reaches the critical pressure. The dimensionless drag can be calculated from **Fig. 3(a)** by using Eq. (6). **Fig. 3(b)** shows the reciprocal of dimensionless drag as a function of Knudsen number, for test filters. It is seen from **Fig. 3(b)** that the reciprocal of dimensionless drag linearly increases with Knudsen number, indicating that the empirical equation by Kirsch et al. (1973) holds for nanofiber filters. However, the slope of  $1/F$  which corresponds to the degree of slip flow does not show any dependence on fiber diameter: the slopes are in the order of NF78 < NF216 < NF99 < NF440 < NF70 < NF157 < NF300 < NF407 as shown in the **Table 2**. The

test filter of NF407 shows the highest slope even though it consists of relatively thick fibers, and the test filter of NF78 consists of relatively fine fiber filter has the lowest slope. This may be attributed to the packing density and inhomogeneity of fiber packing as the previous works reported that the slip flow significantly affected by the inhomogeneity of fiber packing (Kirsch et al., 1973; Bao et al., 2016).

According to the Eq. (2), the slope of  $1/F$  is a function of the packing density and inhomogeneity factor. In order to investigate the influence of packing density on the slip flow, we plotted the slope of  $1/F$  as a function of  $(1 - \alpha)$  in **Fig. 4**. In **Fig. 4** we cannot see any dependence of the slope of  $1/F$  on  $(1 - \alpha)$  because the inhomogeneity of nanofiber filters varies a lot (from 3.87 to 62.2 in Table 2). The nanofiber filters used in the present work were made of various polymers with different methods so that their physical properties such as fiber diameter, packing density, and thickness are different.

In the following section, we investigate the effect of inhomogeneity of fiber packing on the slip flow. **Fig. 5** compares the experimental reciprocal of dimensionless drag of test filter NF70 with the one predicted for FMF by Eq. (4). The discrepancy between the test filter and the FMF represent the degree of inhomogeneity of fibers, and we may calculate the inhomogeneity factor by reading the intercept of ordinate at  $Kn = 0$ . **Table 2** shows the inhomogeneity factor of test filters in the far right column. As seen in the table, the inhomogeneity factors of nanofiber filters studied in the present work ranged from 3.9 to 62.2, which is significantly large compared to the filters studied by Kirsch et al. (1973) ( $\delta = 1.08-2.20$ ). It is noted that the test filter NF407 which has the highest inhomogeneity factor ( $\delta = 62.2$ ) in Table 2 gives the largest slope in **Fig.3** and that the test filter NF78 which has the smallest inhomogeneity factor ( $\delta = 3.9$ ) gives the smallest slope in **Fig.3**, as expected by Kirsch's formula Eq. (2).

We cannot prepare nanofiber filters with different packing densities which have the same inhomogeneity factor, i.e., the same filter structure. Consequently, we would accept the dependence of slope of  $1/F$  on  $(1 - \alpha)$  as proposed by Kirsch's formula, and, in **Fig. 6**, the slope of  $1/F$  divided by  $(1 - \alpha)$  is plotted against the inhomogeneity factor for nanofiber filters. At the same time, the experimental data reported by Kirsch et al. (1973) are also plotted. It is seen from the figure that the data for nanofiber filters fall on the single straight line predicted by Kirsch's formula together with their data. Therefore, we may conclude that the empirical equation reported by Kirsch et al. (1973) is valid and that the slope of  $1/F$  divided by  $(1 - \alpha)$  is proportional to the square root of inhomogeneity factor even for nanofiber filters which have a large value of the inhomogeneity factor.

## 5. Conclusion

In the present work, we collected various commercially-available nanofiber filters, and the pressure drop was measured at low pressures in order to examine the validity of empirical equation proposed by Kirsch et al. (1973). As a result, we found that the empirical equation is valid and the slope of  $1/F$  divided by  $(1 - \alpha)$  is proportional to the square root of inhomogeneity factor even for nanofiber filters which have a large value of the inhomogeneity factor.

## References

- Bao, L., Seki, K., Niinuma, H., Otani, Y., Balgis, R., Ogi, T., Gradon, L., & Okuyama, K. (2016). Verification of slip flow in nanofiber filter media through pressure drop measurement at low pressure conditions. *Separation and Purification Technology*, 159, 100-107.
- Barhate, R. S., & Ramakrishna, S. (2007). Nanofibrous filtering media: Filtration problems and solutions from tiny materials. *Journal of Membrane Science*, 296, 1-8.
- Brown, R. C. (1993). *Air filtration: An Integrated Approach to the Theory and Applications of Fibrous Filters*. Oxford: Pergamon Press.
- Choi, H. -J., Park, E. -S., Kim, J. -U., Kim, S. H., & Lee, M. -H. (2015). Experimental study on charge decay of electret filter due to organic solvent exposure. *Aerosol Science and Technology*, 49, 977-983.
- Hinds, W. C. (1999). *Aerosol Technology: Properties, Behavior, and Measurement of Airborne Particles*. (2nd ed.). New York: Wiley.
- Hung, C. -H., & Leung, W. W. -F. (2011). Filtration of nano-aerosol using nanofiber filter under low Peclet number and transitional flow regime. *Separation and Purification Technology*, 79, 34-42.
- Kirsch, A. A., Stechkina, I. B., & Fuchs, N. A. (1973). Effect of gas slip on the pressure drop in fibrous filters. *Journal of Aerosol Science*, 4, 287-293.
- Leung, W. W. -F., & Hung, C. -H. (2012). Skin effect in nanofiber filtration of submicron aerosols. *Separation and Purification Technology*, 92, 174-180.
- Li, X., Wang, N., Fan, G., Yu, J., Gao, J., Sun, G., & Ding, B. (2015). Electrospun polyetherimide-silica fibrous membranes for enhanced filtration of fine particles. *Journal of Colloid and Interface Science*, 439, 12-20.
- Pich, J. (1971). Pressure characteristics of fibrous aerosol filters. *Journal of Colloid and Interface Science*, 37, 912-917.
- Sambaer, W., Zatloukal, M., & Kimmer, D. (2011). 3D modeling of filtration process via polyurethane nanofiber based nonwoven filters prepared by electrospinning process. *Chemical Engineering Science*, 66, 613-623.
- Wang, C. -S., & Otani, Y. (2013). Removal of nanoparticles from gas streams by fibrous filters: A Review. *Industrial and Engineering Chemistry Research*, 52, 5-17.
- Zhang, Q., Welch, J., Park, H., Wu, C. -Y., Sigmund, W., & Marijnissen, J. C. M. (2010). Improvement in nanofiber filtration by multiple thin layers of nanofiber Mat. *Journal of Aerosol Science*, 41, 230-236.

## **Table Titles**

**Table 1** Physical properties of test filters in the previous work (Kirsch et al., 1973).

**Table 2** Physical properties of test filters and experimental results.

**Table 1** Physical properties of test filters in the previous work (Kirsch et al., 1973).

Test filter	Fiber diameter, $d_f$ [ $\mu\text{m}$ ]	Thickness, $L$ [mm]	Packing density, $\alpha$ [-]	Inhomogeneity factor, $\delta$ [-]
1	14	5.8	0.04	1.39
2	14	3.3	0.07	1.43
3	14	2.3	0.10	1.41
4	14	2.8	0.14	1.40
5	18.1	2.4	0.11	2.03
6	14	2.4	0.03	1.30
7	14	3.5	0.038	1.30
8	13.2	2.4	0.08	2.20
9	7.14	2.1	0.035	1.13
10	7.14	2.5	0.063	1.90
11	3.14	1.5	0.017	1.08

**Table 2** Physical properties of test filters and experimental results.

Test filter	Fiber diameter, $d_f$ [nm]	Thickness, $L$ [mm]	Packing density, $\alpha$ [-]	Slope [-]	Inhomogeneity factor, $\delta$ [-]
NF70	70.0	0.01	0.08	0.328	29.36
NF78	78.3	0.06	0.07	0.135	3.87
NF99	99.4	0.05	0.01	0.175	6.55
NF157	156.8	0.23	0.15	0.334	24.51
NF216	216.3	0.01	0.13	0.174	5.36
NF300	299.6	0.38	0.09	0.438	21.77
NF407	406.5	0.10	0.14	0.744	62.20
NF440	440.0	0.38	0.07	0.246	7.12

## Figure captions

**Fig. 1.** Experimental results in the previous work (Kirsch et al., 1973).

**Fig. 2.** Experimental setup for pressure drop measurement at the low pressures.

**Fig. 3 (a).** Pressure drop of test filters as a function of absolute pressure.

**Fig. 3(b).** Dependence of dimensionless drag on Knudsen number for nanofiber filters.

**Fig. 4.** Dependence of slope of  $1/F$  on  $(1 - \alpha)$  for nanofiber filters.

**Fig. 5.** Comparison between theoretical reciprocal of dimensionless drag of FMF and experimental reciprocal of dimensionless drag for NF70.

**Fig. 6.** Dependence of slope of  $1/F$  divided by  $(1 - \alpha)$  on inhomogeneity factor.

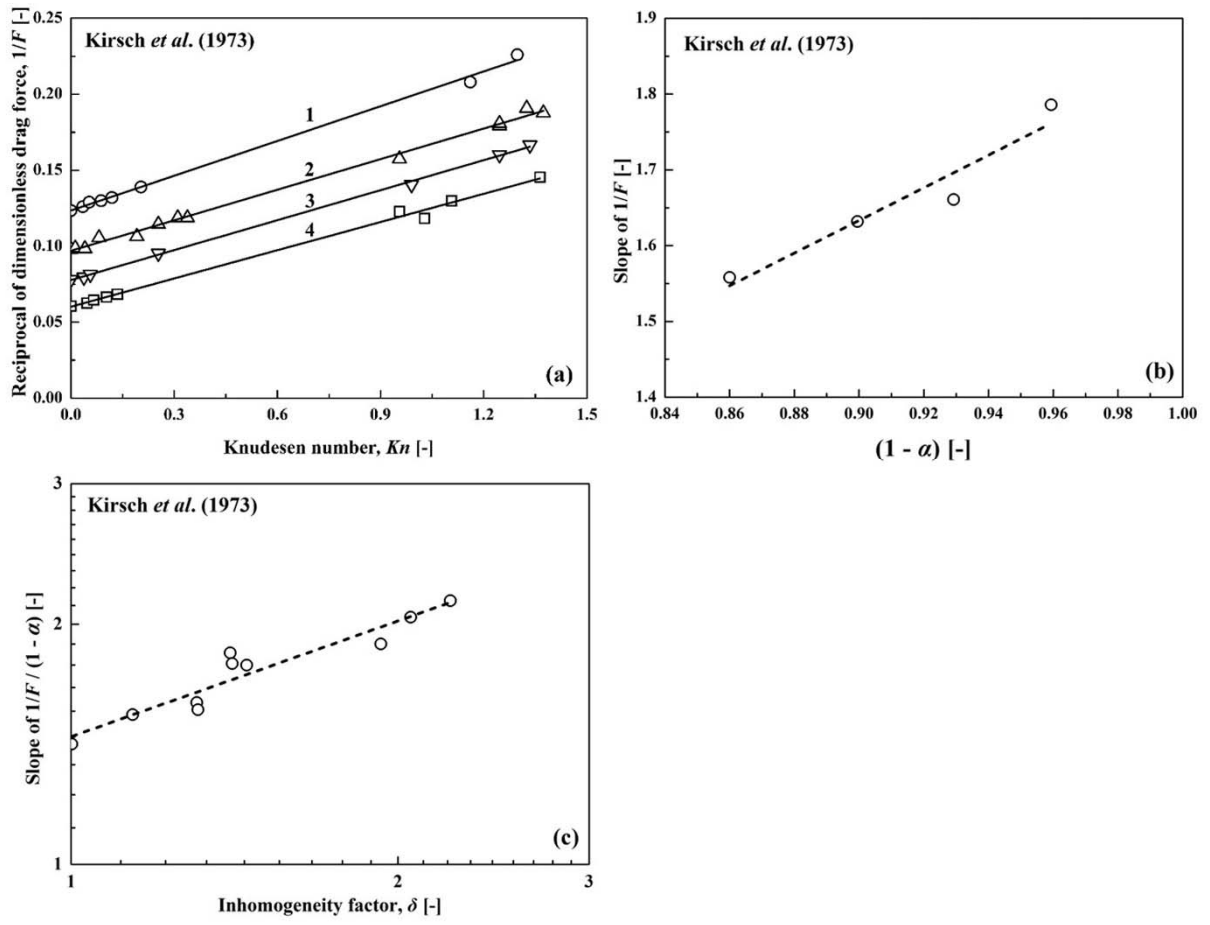


**Fig. 1.**

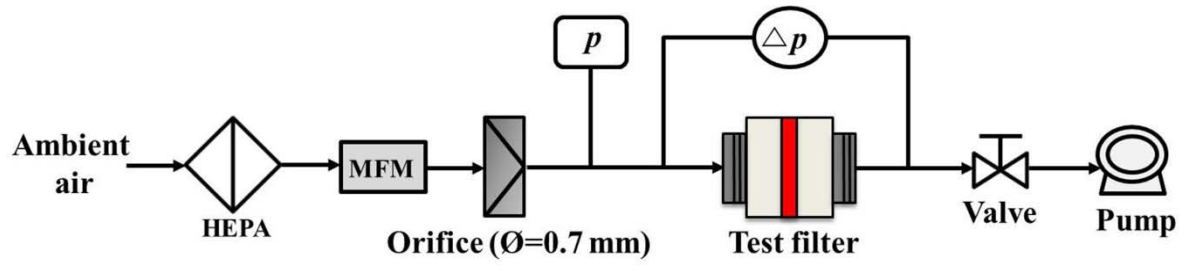


Fig. 2.

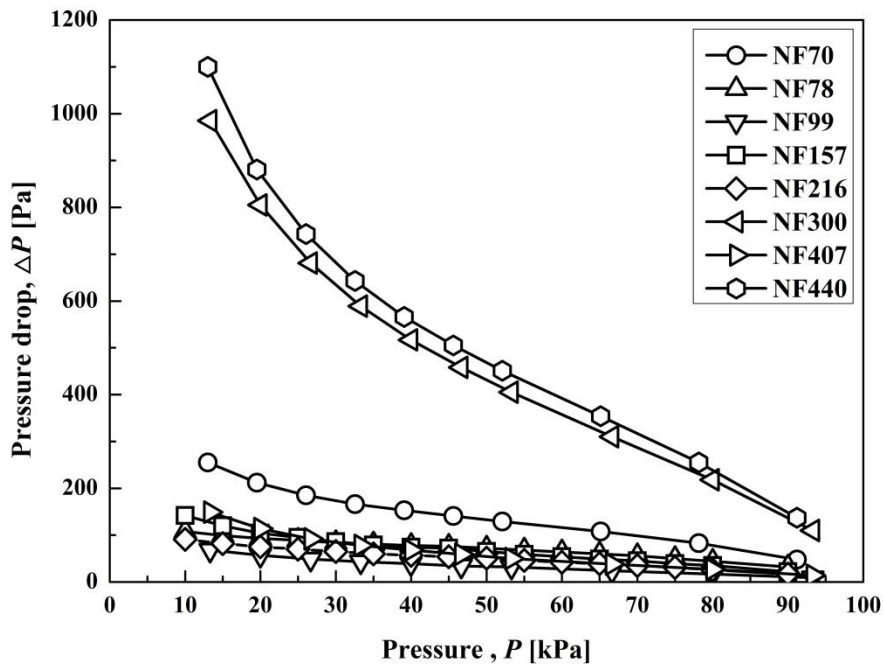


Fig. 3(a).

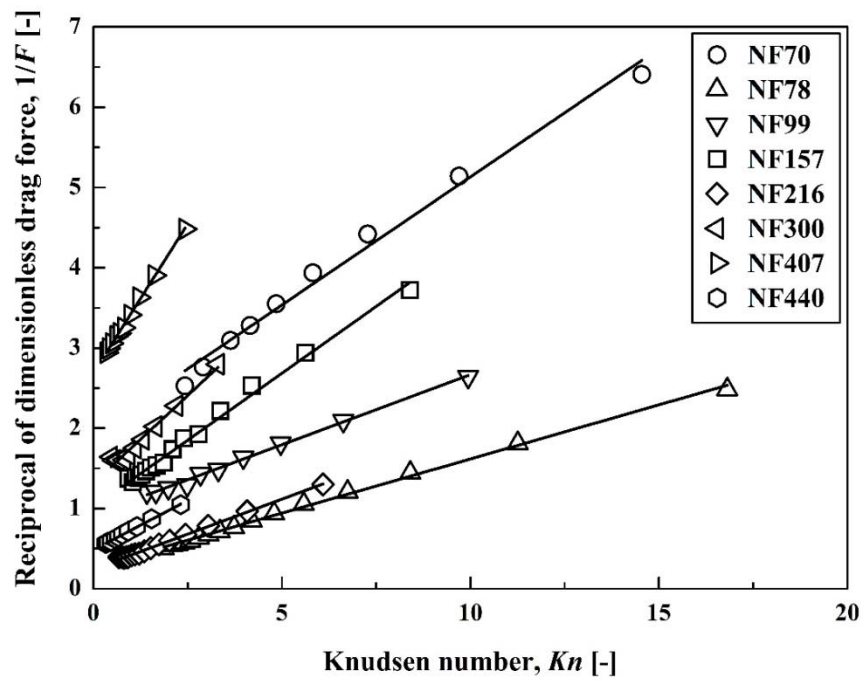


Fig. 3(b).

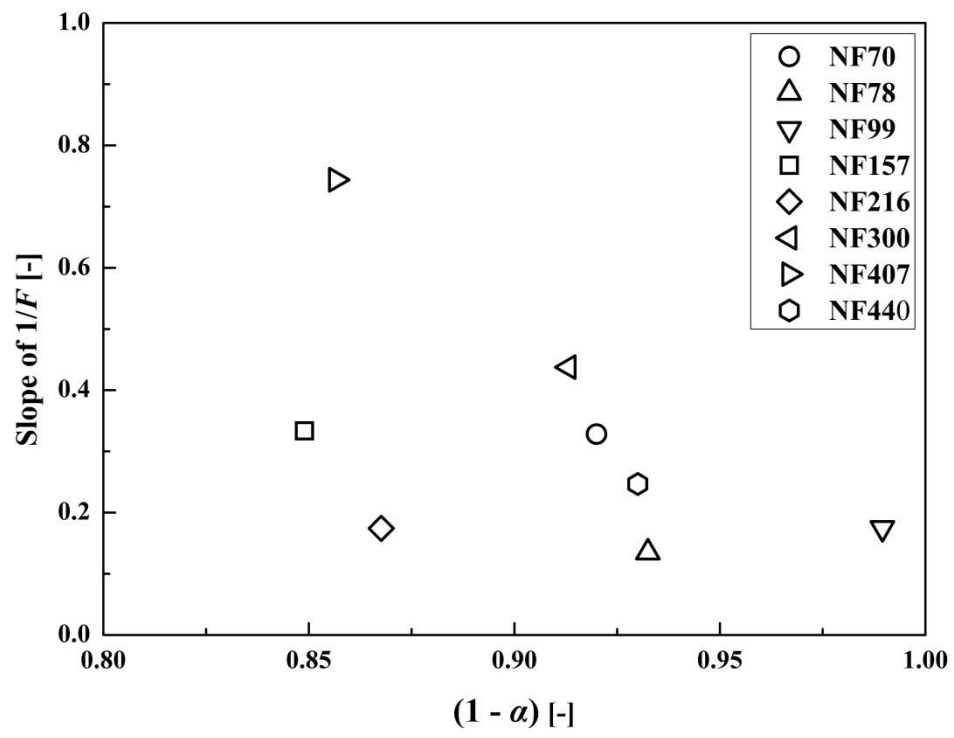


Fig. 4.

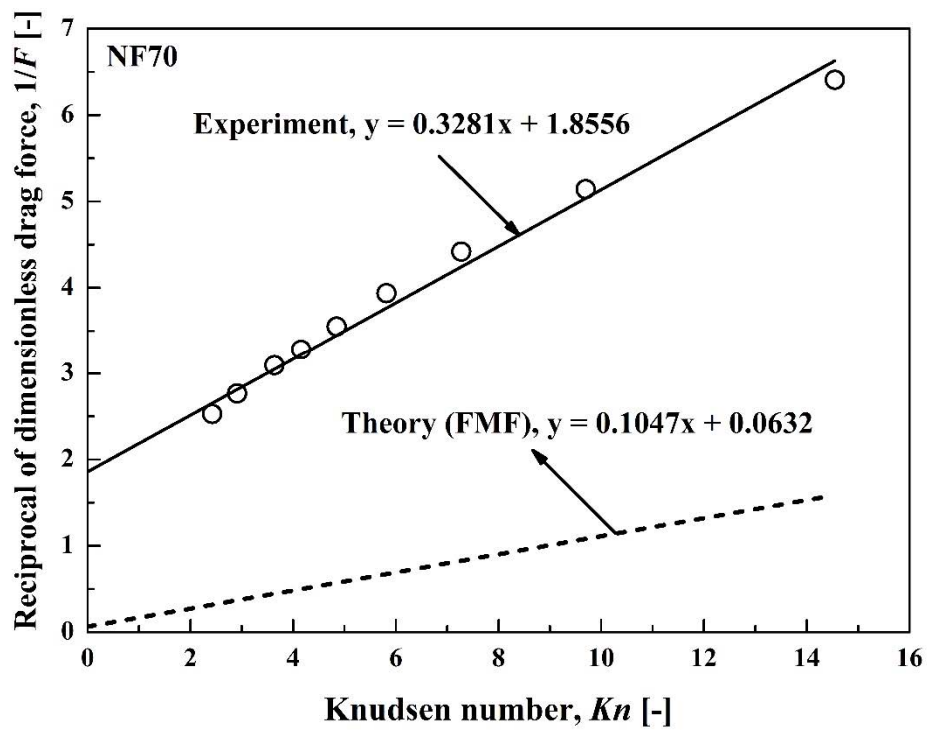


Fig. 5.

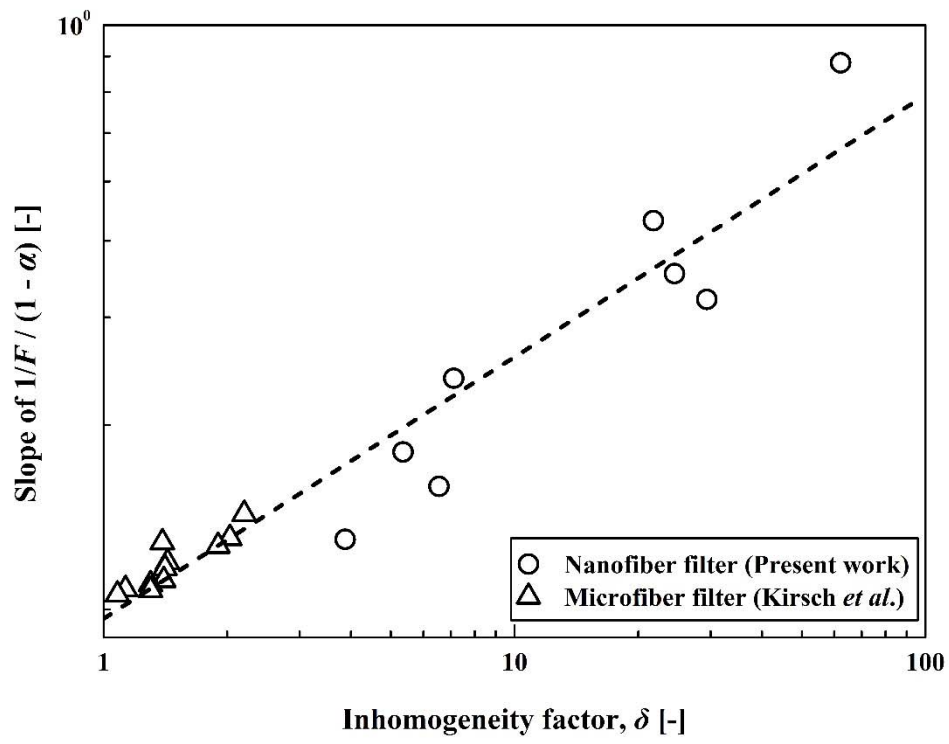


Fig. 6.